# SYNTHESIS AND CHARACTERIZATION OF PURE $\alpha$-$Fe_2O_3$ NANOPARTICLES

Dissertation submitted to

**SRI S. RAMASAMY NAIDU MEMORIAL COLLEGE, SATTUR**

(Re-Accredited with A grade by **NAAC**)

Affiliated to Madurai Kamaraj University

In Partial fulfillment of the requirement for the Degree of

**MASTER OF SCIENCE**

**IN**

**PHYSICS**


**Submitted by**

**Ms. T. BIRUNDHA (PPH205004)**

**Ms. S. NITHYA PRIYA (PPH205016)**


Under the Guidance of


**Dr. P. SUNDARA VENKATESH**
**Assistant Professor**

**DEPARTMENT OF PHYSICS**
**SRI S. RAMASAMY NAIDU MEMORIAL COLLEGE**
**SATTUR – 626203**


**JUNE - 2022**

**Department of Physics**
**Sri S. Ramasamy Naidu Memorial College**
**Sattur-626203, Tamil Nadu**
**E-mail: anitha@srnmcollege.ac.in**
**Mobile: 97901 21260**

**Dr. R. ANITHA**
**Assistant Professor & Head**

**DATE: 10.06.2022**

## CERTIFICATE

This is to certify that this dissertation entitled **"SYNTHESIS AND CHARACTERIZATION OF PURE α-$Fe_2O_3$ NANOPARTICLES"** being submitted by **Ms. T. BIRUNDHA** and **Ms. S. NITHYA PRIYA,** Students of M.Sc., degree course in Physics, **SRI S. RAMASAMY NAIDU MEMORIAL COLLEGE, SATTUR** affiliated to **MADURAI KAMARAJ UNIVERSITY, MADURAI** is a bonafide record of work carried out by them in our department during the academic year 2021-2022.

Signature of the Head of the Department

**[Dr. R. ANITHA]**

**Department of Physics**
**Sri S. Ramasamy Naidu Memorial College**
**Sattur -626203, Tamil Nadu**
**E-mail: srnmcphysics@gmail.com**
**Mobile: 80723 57026**

**Dr P. SUNDARA VENKATESH** **DATE: 10.06.2022**
**Assistant Professor**

## CERTIFICATE

This is to certify that this dissertation entitled **"SYNTHESIS AND CHARACTERIZATION OF PURE $\alpha$-$Fe_2O_3$ NANOPARTICLES"** being submitted by **Ms. T. BIRUNDHA** and **Ms. S. NITHYA PRIYA,** Students of M.Sc., degree course in Physics, **SRI S. RAMASAMY NAIDU MEMORIAL COLLEGE, SATTUR** affiliated to **MADURAI KAMARAJ UNIVERSITY, MADURAI** is a bonafide record of work carried out by them under my guidance and supervision during the academic year 2021 - 2022.

Signature of the Guide

**Dr. P. SUNDARA VENKATESH**

**Department of Physics**
**Sri S. Ramasamy Naidu Memorial College**
**Sattur -626203**
**Tamil Nadu**

**DATE: 10.06.2022**

## DECLARATION

The dissertation entitled **SYNTHESIS AND CHARACTERIZATION OF PURE α-$Fe_2O_3$ NANOPARTICLES** being submitted by **Ms. T. BIRUNDHA** and **Ms. S. NITHYA PRIYA** Students of M.Sc., degree course in Physics, **SRI S. RAMASAMY NAIDU MEMORIAL COLLEGE, SATTUR** affiliated to **MADURAI KAMARAJ UNIVERSITY, MADURAI** in partial fulfillment of the requirement for the Degree of Master of Science.

We further declare that this dissertation or any part of this project has not been submitted to this university or elsewhere for any other degree or diploma.

Signature of the Students

Ms. T. BIRUNDHA

Ms. S. NITHYAPRIYA

## ACKNOWLEDGEMENT

We pay our deep sense of gratitude to the lord almighty for giving us strength for the completion of this project.

We also express my sincere thanks to **Dr. R. ANITHA** Head of the department of PG Physics for providing full freedom to undertake this project. I immensely thank him for her overall help, support, and guidance at all the stages.

We are much privileged to have **Dr. P. SUNDARA VENKATESH**, as a guide, Assistant Professor, Department of UG Physics. We would like to express our sincere thanks to him for his constant support, motivation, and valuable suggestions in all our endeavors.

We would like to **thank Mr. KANNAN, Ms. S. SAISREE, and Ms. UMASANKARI, Research Scholars** of Nanomaterials Laboratory, Department of Physics for their innovative suggestions, and immense support in completing the project successfully.

We express our grateful thanks to the faculty members

**Ms. K. THILAGA, Ms. R. LATHA, Dr. P. LAKSHMANA PERUMAL, and Ms. R. PRIYANGA** of our department.

Last but not least, we take this opportunity to thank my beloved Parents without them we would not be here.

Ms. T. BIRUNDHA

Ms. S. NITHYAPRIYA

## CONTENT

# CHAPTER - I

## 1.1 Introduction of nanomaterials

Nanomaterials are commonly defined as materials with an average grain size of less than 100 nm. Nanomaterials have an extremely small size having at least anyone of the dimensions less than 100 nm. One billion nanometers is equal to one meter. Nanomaterials are any type of material that of nanosized in dimension. These nanomaterials are classified into Zero dimension (0D), one dimension (1D), or two dimensions (2D) based on their dimensions.

In zero-dimension (0D) nanomaterials, all three dimensions are measured within the nanometer scale. An example of 0D nanomaterials is nanoparticles. In 1D nanomaterials, 1D is on a large scale and other 2D are on the nanometer scale. This includes a nanotube, nanorods, and nanowires. In 2D nanomaterials, two dimensions are on the large scale and 1D is on a nanometer scale. This exhibits plate-like shapes which include graphene and other monolayer materials such as black phosphorous and diatomic hexagonal boron nitride.

Various metal oxide nanoparticles have been synthesized by different preparation methods. Among them, the narrow bandgap metal oxide nanoparticles ($BiVO_4$, $Fe_2O_3$, CdO) have received tremendous interest in the field of photocatalytic dye degradation and photocatalytic water splitting owing to the light absorption in the visible region of the electromagnetic spectrum. In this narrow bandgap semiconducting metal oxides, $Fe_2O_3$ nanoparticles due to its unique properties.

## 1.2 Introduction to $\alpha$ - $Fe_2O_3$

Iron oxides or ferric oxide is an inorganic compound with the formula $Fe_2O_3$. Iron oxide is a reddish-brown solid. The red color is referred to as venetian red. $Fe_2O_3$ is ionic. The oxidation state of +3 and +2. The bond formed between iron and oxygen is because of difference in electronegativity between two atoms. Hence, the iron is metal and the oxygen is non-metal the bonding between iron and oxygen is ionic.

Iron oxides are composed of iron and oxygen. There are various types of iron oxides such as iron (II) oxides, iron (III) oxides ($Fe_2O_3$), alpha phase, magnetite ($Fe_3O_4$), hematite ($\alpha$-$Fe_2O_3$), $\beta$-$Fe_2O_3$ and $\gamma$-$Fe_2O_3$ whereas $\alpha$-$Fe_2O_3$ is most important and stable metal oxide of all forms.

The mineral name of $\alpha$-$Fe_2O_3$ iron oxide is hematite. It exists in rhombohedral corundum structure in common. Molecular weight of iron oxide is 159.69 g/mol. The iron oxide density is 5.242 $g/cm^3$. The melting point is 1475-1565°C When boiled $\alpha$-$Fe_2O_3$ gets thermally decomposed. Its bandgap is 2.2-2.4eV. $\alpha$-$Fe_2O_3$ has photocatalytic because of a suitable band gap for absorption in the visible region, biocompatibility, easy availability, low cost, and stability in aqueous solutions.

A photocatalytic activity is a reaction that happens in the presence of light, it is meant to be activating the photocatalyst in the presence of visible light or UV- light. A photocatalytic material could be a semiconductor as it has the ability to generate electrons and holes when exposed to light. The steps of a photocatalytic reaction involve the absorption of light by a semiconductor material followed by an electron transfer from the valence band (VB) to the conduction band (CB) creating a hole in the VB. The VB and CB are separated by some energy barrier called the band gap ($E_g$).

$\alpha$-$Fe_2O_3$ has been widely used in the photodegradation of dyes and organic contaminants. The degradation of dyes and organic pollutants over $\alpha$-$Fe_2O_3$ by the photocatalytic reaction is scanty [1]. The principle of the photocatalytic mechanism is the absorption of incident photons with energy above or equal to the band gap of photocatalyst, generating photoexcited electrons at CB and the same number of holes at VB. These electrons and positive holes are involved in the reduction and oxidation, respectively. The produced holes abstract electrons from absorbed pollutants or react with $H_2O$ to form $OH^-$. On the other hand, the CB electrons reduce the absorbed oxygen to form $O2^-$. α-Fe2O3 can also form composites with wide band gap materials like ZnO [2], and $TiO_2$ [3] forming the Z-scheme heterojunction.

# CHAPTER - II

# PREPARATION AND CHARACTERIZATION TECHNIQUES

**Preparation methods**

## 2.1 Preparation methods

Nanomaterials can be prepared from a variety of materials such as metals, semiconductors, insulators, dielectrics, etc., and for this purpose, various preparative techniques have also been developed. A variety of deposition techniques can be employed to fabricate nanomaterials. The few preparation techniques are

1. Hydrothermal Method
2. Co-precipitation Method
3. Chemical Vapor Deposition (CVD)
4. Sol-gel Method

### 2.1.1 Hydrothermal method

The hydrothermal method is a chemical reaction in water in a sealed pressure vessel, in fact, a type of reaction at both high temperature and pressure. Hydrothermal synthesis is a commonly used method for nanoparticle preparation. It is a solution reaction-based approach. The formation of nanomaterials in wide temperature ranges from room temperature to very high temperature [4].

### 2.1.2 Co-precipitation method

The co-precipitation method involves the precipitation of metal in the form of hydroxide from a salt precursor with the help of a base in a solvent. Advantages of simple and rapid preparation, easy control of particle size and composition, where it is possible to modify the particle surface state and overall homogeneity. There are four types of co-precipitation, they are surface adsorption, mixed-crystal formation, occlusion, and mechanical entrapment [5].

### 2.1.3 Chemical Vapor Deposition method

Chemical vapor deposition is a process in which the substrate is exposed to one more volatile precursor versus in which reactions are decomposed on the substrate surface to produce the thin film industries such as coatings. In coatings such as wear resistance, corrosion resistance, high-temperature protection, and erosion protection [6].

### 2.1.4 Sol-gel method

A sol-gel process involves the evolution of inorganic networks through the formation of a colloidal suspension (sol) and gelation of the sol to form a network in a continuous liquid phase (gel). It is used in process of making ceramics as a molding material and used as an intermediate between thin films of metal oxide in various applications. Among all the above methods sol-gel method is of low cost, and easy to prepare [7].

## 2.2 Characterization techniques

### 2.2.1 X - ray diffraction (XRD)

XRD analysis is a technique used in materials science to determine the crystallographic structure of a material. It is working on the principle of constructive interference of monochromatic X- rays. X-rays are produced in a cathode tube and allowed to interact with the crystals. The X-rays get diffracted by a crystal because the wavelength of X- rays is similar to the inter-atomic spacing in the crystals. These scattered X-rays produce constructive interference according to the Bragg's law ($n\lambda = 2d \sin\theta$). The Bragg's diffractions occur when the wavelength of radiation is comparable to the atomic spacing in a crystalline sample. These diffracted X-rays are detected and then processed. Fig. 2.1 shows the schematic representation of X-ray diffraction.

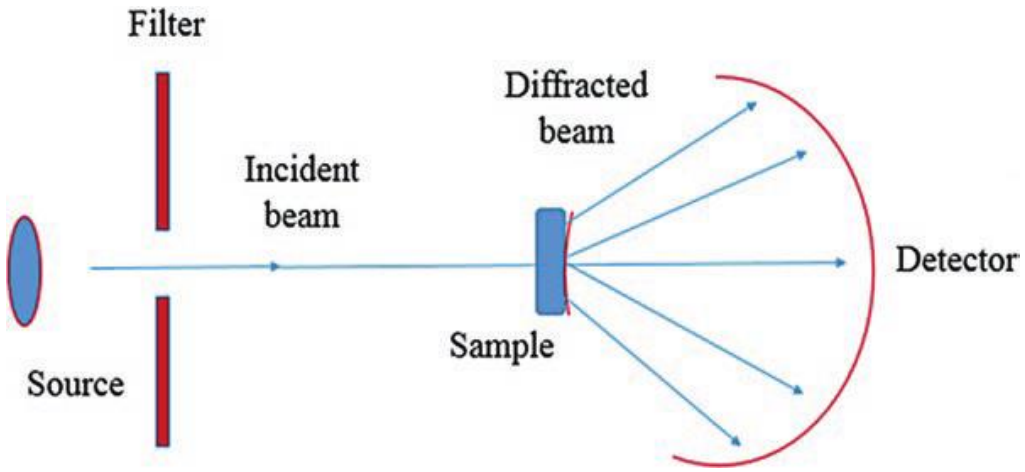


**Fig 2.1 A schematic diagram of X-Ray Diffraction**

### 2.2.4 SCANNING ELECTRON MICROSCOPY (SEM)

The first commercial model of SEM was developed by the Cambridge Scientific Instrument Company in UK in the year 1965. Since then, several models of SEM are in use in several research institutes all over the world.

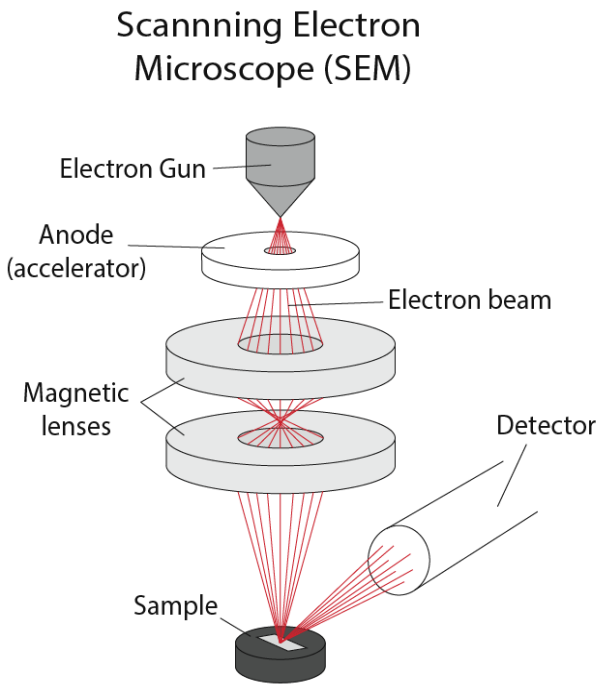


**Fig 2.2 A schematic diagram of scanning electron microscope**

SEM provides information relate to the morphology distribution. SEM is also capable of determining the elemental composition of micro volumes. Because of the high resolution, good quality of microphotograph can be obtained by the SEM. Another important feature of the SEM is the three-dimensional appearances of specimen image. This three-dimensional appearance is a direct result of the large depth of focus frequency an X-ray received for each energy level. An EDAX spectrum normally display peaks corresponding to the energy levels for which the most of the X-rays have been received. Each of these peaks is unique to an atom and therefore corresponds to a single element. The height of a peak in a spectrum indicates the concentration of the element in the specimen. An EDAX spectrum plot not only identifies the element corresponding to each of its peaks, but also the type of X-ray to which it corresponds as well.

### 2.2.5 **Raman spectroscopy**

Raman spectroscopy is a spectroscopic technique that is typically used to determine vibrational modes of molecules, although rotational and other low-frequency modes of the system. Raman Spectroscopy is based on scattering. This sample is irradiated with a coherent source, typically a laser. Most of the radiation is elastically scattered. A small portion is inelastically scattered. It is called Raman scattering and it is composed of stokes and anti-stoke lines.

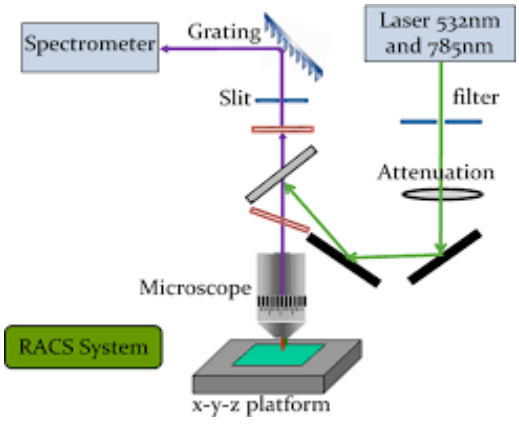


**Fig 2.3 shows the working of a Raman spectrometer**

## 2.2. UV-visible spectroscopy

UV - visible spectroscopy is used to determine the absorption or transmission of UV - visible light by a sample. It can also use to measure the concentration of absorbing materials based on developed calibration curves of the material. A spectrometer is employed to measure the amount of light that a sample absorbs. The instrument operates by passing a beam of light through a sample and measuring the intensity of light reaching a detector. The beam of light consists of a stream of photons. When a photon encounters an analytic molecular, there is a chance the analytic will absorb the photon. This absorption reduces the number of photons in the beam of light, thereby reducing the light beam. UV - Visible is a form of electromagnetic radiation with a wavelength from 10 to 400 nm shorted than that of visible light. The sample is placed in the UV - Visible beam and a graph of the absorbance versus the wavelength is obtained. The energy band is determined from this spectrum.

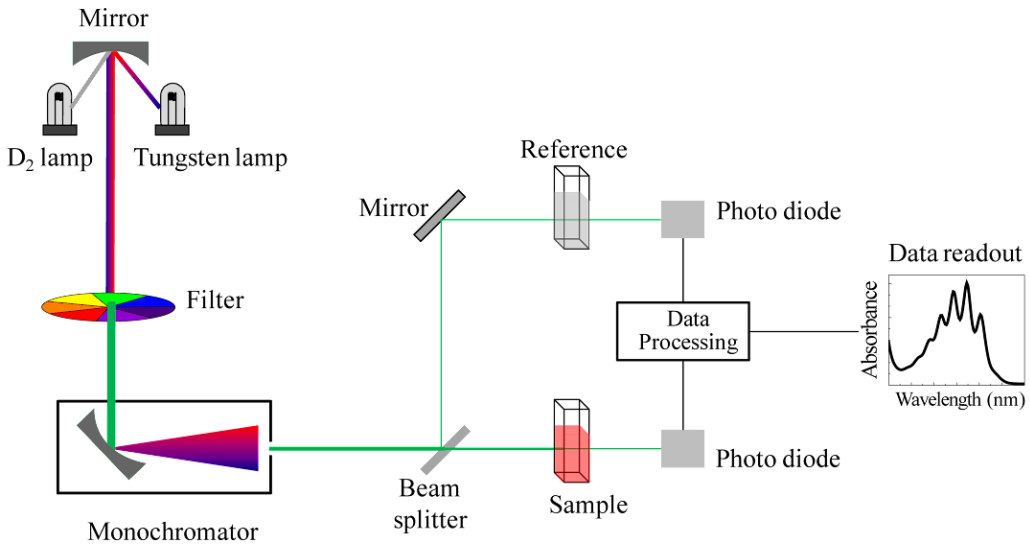


**Fig.2.2 Working of a UV-Vis. Spectrophotometer**

# CHAPTER - III

# EXPERIMENTAL METHOD

# PREPARATION OF $\alpha$-$Fe_2O_3$ NANOPARTICLES

## 3.1 Sol-gel synthesis

Sol-gel synthesis is one of the most commonly used bottom-up approaches in material synthesis. The metal alkoxide is dissolved in an organic solvent to form a homogeneous solution with the addition of chelating agents. The sol-gel method involves several steps.

1. Hydrolysis and polycondensation.
2. Gelation
3. Aging
4. Drying
5. Densification
6. Crystallization

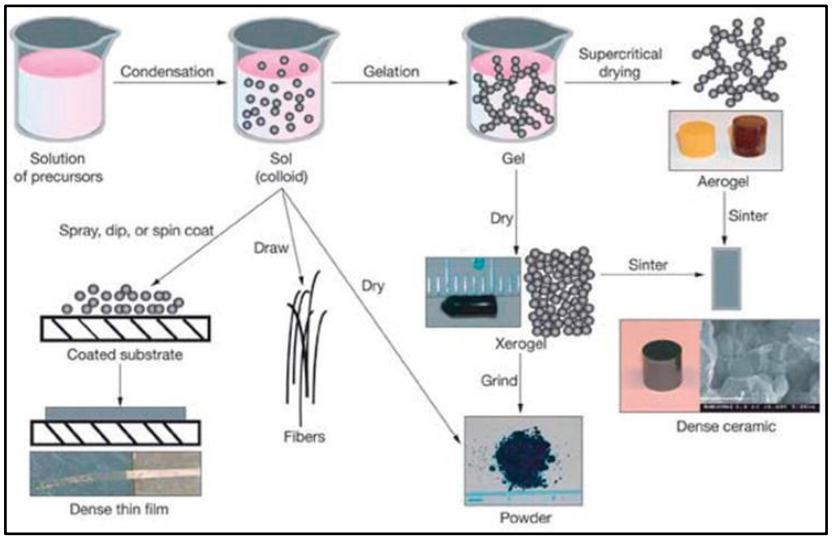


**Fig 3.1 shows the schematic diagram of the sol-gel method**

Sol-gel helps in preparing nanoparticles with uniform size distribution. Sol is a colloidal suspension of particles of size around 1-1000 nm, which are in constant Brownian motion, held

only by weak forces such as van der Waals attraction force. A “gel” is a continuous liquid phase extended as a three-dimensional network usually by interlinked polymeric chains. The colloidal gel is mostly an agglomeration of covalently bonded particles wherein the gel formation is reversible. Sol-gel process starts with hydrolysis, followed by condensation of the precursor to form a gel continued to ageing, solvent extraction and finally drying. The reaction can be catalyzed by addition of an acid or/and a base. The process of drying involves evaporation of water molecules under constant temperature, pressure, and humidity. The dried gel is calcined to get the crystalline material after undergoing reactions such as desorption of solvent and water from the walls of the micropores (100-200 ℃), collapse of small pores (300-400 ℃), collapse of large pores (700-900 ℃) and continued polycondensation gives us the nanoparticles of the desired compound [8].

### 3.2 Synthesis of α-$Fe_2O_3$ nanoparticles

Iron nitrate anhydrate (Fe $(NO)_3)_2$.6. $H_2O$ was purchased in pure form from Merck. 0.1M of iron nitrate precursor is taken in double-distilled water and stirred for 10 min in a magnetic stirrer and the substrate in which the iron nitrate precursor is to be added is a gelatin matrix made with 0.1M of gelatin powder dissolved in water with stirring in magnetic stirrer followed by heating until it gives the clear solution. Add the iron nitrate solution to the gelatin solution. The solution is placed in a hot plate with continuous stirring for 3 hours. After that the magnetic peddle was removed and heated for 3 hours gives the porous structure of the dried sample. The sample is let to cool down for a day and grinded with a mortar pestle to get the as-prepared sample. The as-prepared sample is annealed at 1000℃ to get brownish-grey α-$Fe_2O_3$ nanoparticles.

# CHAPTER – IV

# RESULTS AND DISCUSSION

## 4.1 Structural studies of α-$Fe_2O_3$ nanoparticles

X-ray diffraction is a very important experimental technique that has been related to the crystal structure of solids, including lattice constants and geometry, identification of unknown materials etc., It must satisfy the Bragg's relation,

$$2d\sin\Theta = n\lambda$$

Where d is interplanar spacing, θ is the angle of diffraction, λ is the wavelength and n is the order of diffraction. Fig. 4.1 shows the XRD pattern of α-$Fe_2O_3$ nanoparticles.

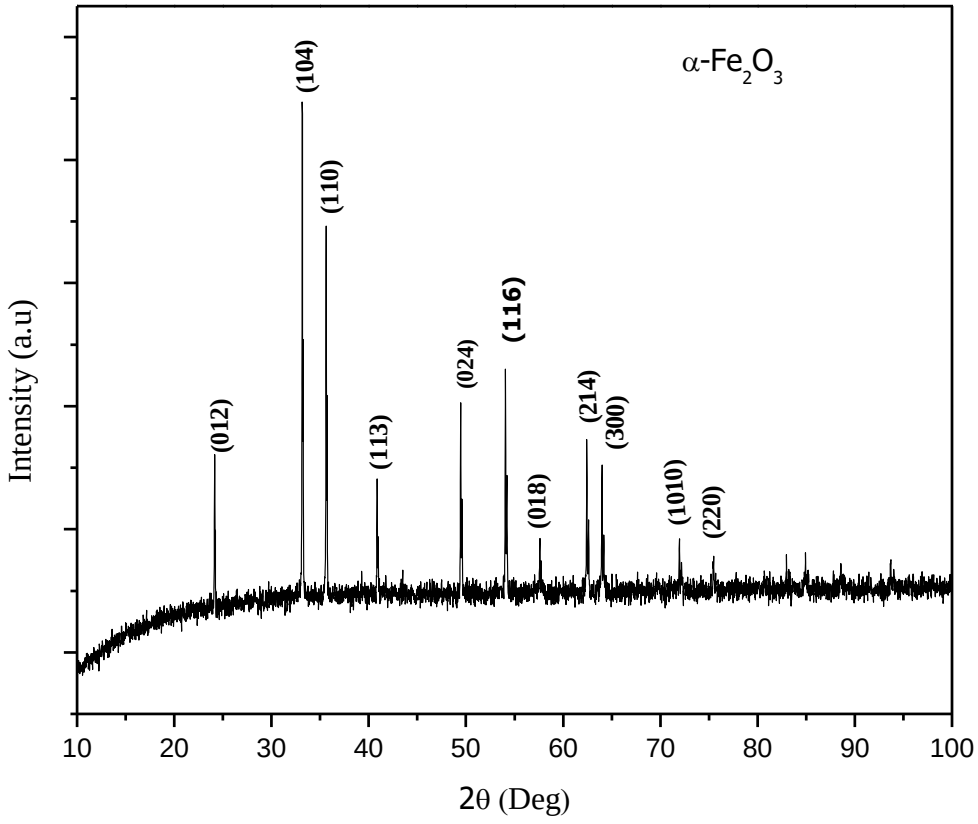


**Fig 4.1 shows the X-ray Diffraction Pattern of α-$Fe_2O_3$ nanoparticles**

The diffraction peaks well match with a Rhombohedral structure of α-$Fe_2O_3$ (JCPDS Card no- 00-033-0664) are indexed respectively as (012), (104), (110), (113), (024), (116), (018), (214), (300), (1010) and (220) crystal planes. XRD pattern of pure α-$Fe_2O_3$ nanoparticles has a predominant peak at ~ $33^0$ which corresponds to (104) orientation.

### 4.2 Morphological study of α-$Fe_2O_3$ nanoparticles

Fig. 4.2 shows the SEM images of $Fe_2O_3$ nanoparticles. The particle size of α-$Fe_2O_3$ nanoparticles has been found using Image J software and it varies from 47 to 68 nm in diameter. Further, the images clearly depict that the nanoparticles are agglomerated which is attributed to the post-annealing of the nanoparticles at 1000 °C.

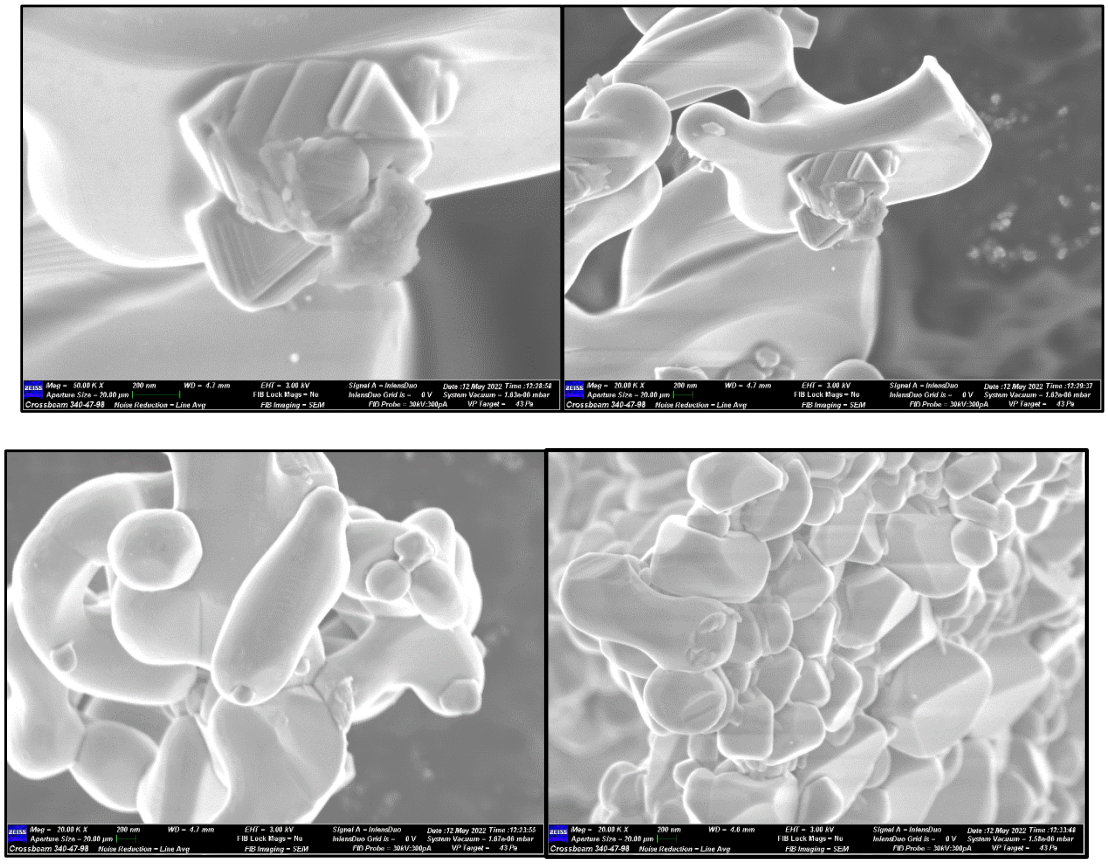

**Fig.4.2 SEM images of α-$Fe_2O_3$ nanoparticles**

### 4.3 Optical study of α-$Fe_2O_3$ nanoparticles

Raman spectroscopy is a non-destructive chemical analysis technique that provides detailed information about chemical structure, phase, polymorphs, crystalline, and molecular interaction. It is based upon the interaction of light with the chemical bonds within a material. Raman Shift is the difference in frequency between the incident light and the scattered light. This difference is unrelated to laser wavelength and expressed as wavenumbers.

Fig. 4.3 shows the Raman spectrum of α-$Fe_2O_3$ nanoparticles. The observed peaks at 220, 2442, 288, 409.3, 493.4, and 604 $cm^{-1}$ are attributed to the $A_{1g}$ and $E_g$ modes of pure α-$Fe_2O_3$

nanoparticles. The observed Raman shift was completely consistent with the previous literature [9].

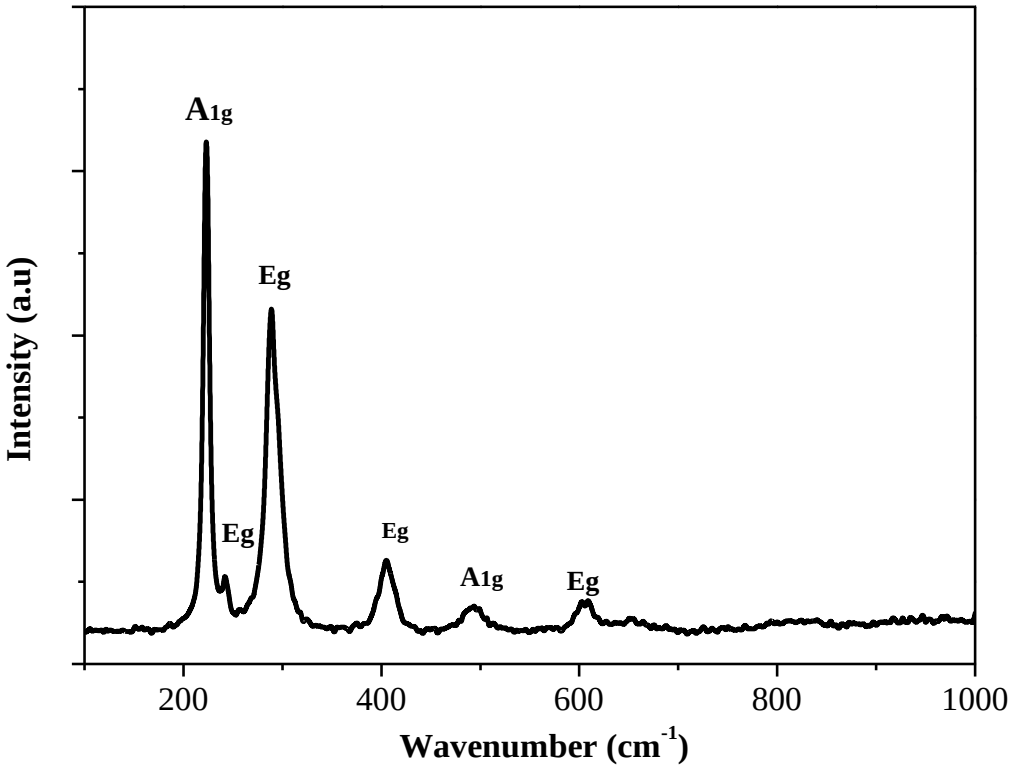


**Fig 4.3 Micro Raman spectrum of Pure α-$Fe_2O_3$ nanoparticles**

### 4.4 Photocatalytic dye degradation of α-$Fe_2O_3$ nanoparticles

The photocatalytic performance of α-$Fe_2O_3$ nanoparticles was studied by using an aqueous solution of methylene blue (MB) and shown in Fig. 4.4. The photocatalytic experiments were carried out under natural sunlight. The initial concentration of the solution was 10 ppm, prepared by dissolving 0.005 mg Methylene Blue [(MB, $C_{16}H_{24}CN_3O_3S$), molecular weight = 373.896 g/mol)] in 250 mL double distilled water. The pH of the solution was kept at 7. The experiments were carried out by mixing 0.1 mg/0.5L photocatalyst in 10 ppm MB dye solution. The subsequent degradation of methylene blue was investigated in the natural sunlight. The degradation of methylene blue was analyzed using a UV–Vis spectrophotometer. The intensity

of predominant absorption band observed at 665 nm quenches with irradiation time. The amount of methylene blue degradation at time t was estimated using the equation:

Degradation = degradation % = $[(C_o - C_t)/ Co] \times 100$

where $C_o$ and $C_t$ refer to the concentration at t = 0 and at time t respectively. The value of methylene blue concentration after degradation was calculated/deduced from the calibration curve.

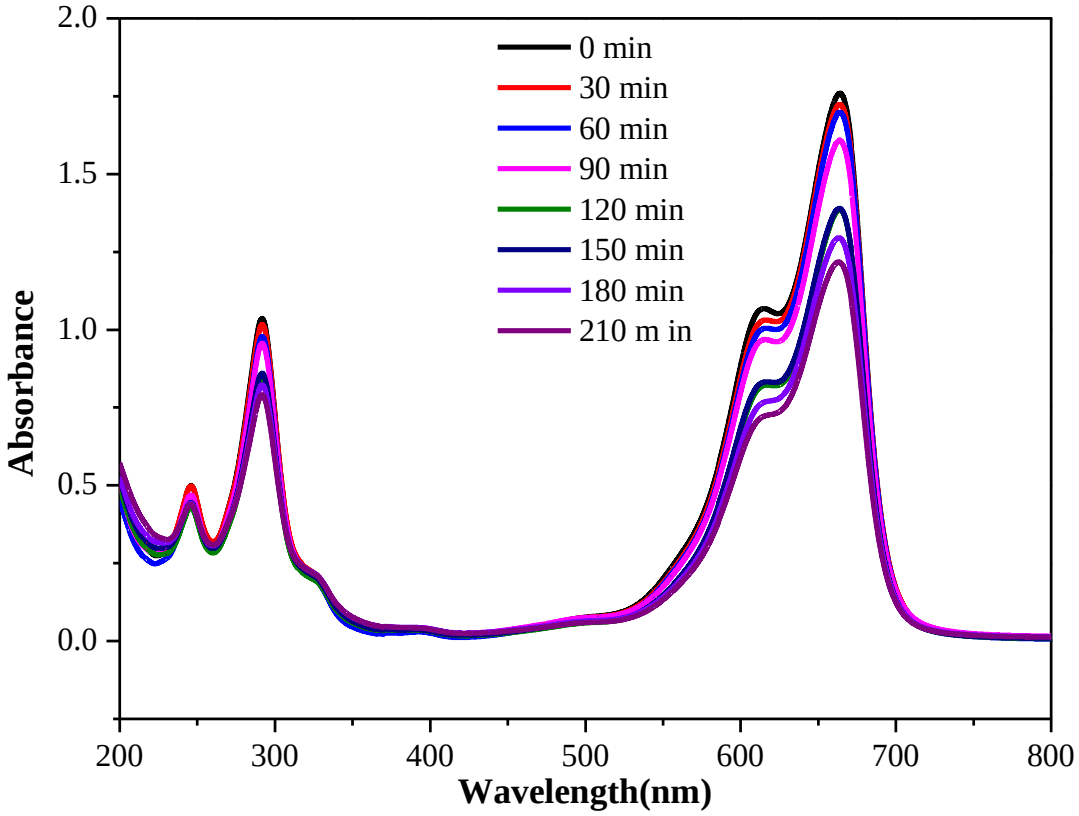


**Fig 4.4 Photocatalytic dye degradation studies of α-$Fe_2O_3$ nanoparticles**

# CHAPTER – V

# CONCLUSION

We have successfully prepared pure α-$Fe_2O_3$ nanoparticles by a sol-gel method. XRD spectrum shows a Rhombohedral structure with $R_3C$ space group. From SEM images, it is clear that the hexagonal-Rhombohedral lattice arrived with plates got agglomerated and disordered. The Raman analysis has interpreted that the sample α-$Fe_2O_3$ has shown all of the vibrational modes as given in the literature. The dye degradation studies of pure α-$Fe_2O_3$ nanoparticles were found to be satisfactory with the low concentration of photocatalyst.

## REFERENCE


1. Maneesha Mishra, and Doo-Man Chun, α-$Fe_2O_3$ as a photocatalytic material: A Review, Applied Catalysis A: General, 498, 2015, 126-141.
2. Dilip K.L. Harijan, Sakshi Gupta, Sachin Kumar Ben, Amit Srivastava, Jai Singh, and Vimlesh Chandra, High photocatalytic efficiency of α-$Fe_2O_3$-ZnO using solar energy for methylene blue degradation, Physica B: Condensed Matter, 627, 2022, 413567.
3. Renji Rajendran, Shanmugam Vignesh, Vairamuthu Raj, Baskaran Palanivel, Atif Mossad Alid, M.A. Sayedd, and Mohd. Shkird, Designing of TiO2/α-$Fe_2O_3$ coupled g-$C_3N_4$ magnetic heterostructure composite for efficient Z-scheme photo-degradation process under visible light exposures, Journal of Alloys and Compounds, 894, 2022, 162498.
4. Marin Tadic, Matjaz Panjan, Vesna Damnjanovic, and Irena Milosevic, Magnetic properties of hematite (-Fe2O3) nanoparticles prepared by hydrothermal synthesis method, Applied Surface Science, 320, 2014, 183-187.
5. Pratibha Sharma, Shikha Dhiman, Sujata Kumari, Pooja Rawat, Chandramohan Srivastava, Hiroki Sato, Takashiro Akitsu, Shalendra Kumar, Imtaiyaz Hassan and Sudip Majumder, Revisiting the physiochemical properties of Hematite (α-$Fe_2O_3$) nanoparticle and exploring its bio-environmental application, Materials Research Express, 6, 2019, 095072.
6. Nurul Affiqah Arzaee, Mohamad Firdaus Mohamad Noh, Azhar Ab Halim, Muhammad Amir Faizal Abdul Rahim, Nurul Aida Mohamed, Javad Safaei, Amin Aadenan, Sharifah Nurain Syed Nasir, Aznan Fazli Ismail, Mohd Asri Mat Teridi, Aerosol-Assisted Chemical Vapor Deposition of α-Fe2O3 Nanoflowers for Photoelectrochemical Water Splitting, Ceramics International, 45, 2019, 16797-16802.
7. Luis T Quispe, L G Luza Mamani, A Baldárrago-Alcántara, L León Félix, Gerardo F Goya, J A Fuentes-García, D G Pacheco-Salazar, and J A H Coaquira, Synthesis and characterization of α-$Fe_2O_3$ nanoparticles showing potential applications for sensing quaternary ammonium vapor at room temperature, *Nanotechnology*, 33, 2022, 335704.

8. Sol-Gel Science, The Physics and Chemistry of Sol-Gel Processing, C Jeffrey Brinker, and George W Scherer, Academic Press Inc.
9. Craig P. Marshall, William J.B. Dufresne, and Carson J. Rufledt, Polarized Raman spectra of hematite and assignment of external modes, Journal of Raman Spectroscopy, 51, 2018, 1522-1529.